J. Fluid Mech. (1993), *vol.* 254, *pp.* 635–648

Shallow-water approach to the circular hydraulic jump

By TOMAS BOHR[1], PETER DIMON[1] AND VAKHTANG PUTKARADZE[1,2]

[1] The Niels Bohr Institute, Blegdamsvej 17, DK-2100 Copenhagen, Denmark

[2] Moscow Physico-Technical Institute, Institutsky per. 9, 141700 Moscow (Dolgoprudny), Russia

(Received 17 March 1992 and in revised form 16 February 1993)

We show that the circular hydraulic jump can be qualitatively understood using simplified equations of the shallow-water type which include viscosity. We find that the outer solutions become singular at a finite radius and that this lack of asymptotic states is a general phenomenon associated with radial flow with a free surface. By connecting inner and outer solutions through a shock, we obtain a scaling relation for the radius R_j of the jump, $R_j \sim Q^{\frac{5}{8}}\nu^{-\frac{3}{8}}g^{-\frac{1}{8}}$, where Q is the volume flux, ν is the kinematic viscosity and g is the gravitational acceleration. This scaling relation is valid asymptotically for large Q. We discuss the corrections appearing at smaller Q and compare with experiments.

1. Introduction

The circular hydraulic jump appears when a vertical jet of fluid is directed upon a horizontal surface and spreads out radially. At a certain radius one observes a sudden increase in the height of the fluid, the mean position of which does not change with time. It is a striking and familiar phenomenon easily observed in a kitchen sink, for example. Nevertheless, there does not seem to be any simple theory which can explain the origin of the jump or give a reasonable estimate of the radius at which it occurs.

In his famous paper on shocks in channel flow (river bores), Lord Rayleigh (1914) shows that continuity of mass and momentum flux across the shock is enough to determine v (the flow velocity along the channel) and h (the height of the fluid) after the jump if they are known before the jump. Consequently, the energy is apparently not conserved across the jump. The lack of energy conservation is usually attributed to dissipation in the jump region and to turbulence generated after the jump.

The radial flow of an ideal fluid has two different steady states which, for large radius r, behave as $v \sim \text{const}\,(h \sim 1/r)$ and $v \sim 1/r\,(h \sim \text{const})$. It is thus tempting to regard the jump as a 'kink' connecting these two states, and it is in fact possible to fit a shock (a discontinuous kink) between them just as in the linear case mentioned above. There is, however, an important difference between channel flow and radial flow. In the former, the shock always propagates, whereas in the latter, the position is fixed although it may fluctuate. Continuity of mass flux and momentum flux is possible at any radius and thus, in the radial case, one more condition is needed in order to determine the radius of the jump. This extra condition could, for example, be the magnitude of the energy loss across the jump, but we know of no simple expression for this quantity. As we shall see below, we believe that such an expression should contain the viscosity in an essential way.

One might question whether it is reasonable that the jump radius should depend strongly on the viscosity. One has to remember, however, that the fluid layer before the jump becomes very thin and will therefore be subjected to a large shear stress. In fact, one can study simple generalizations of shallow-water theory in which the viscous stresses are taken into account in an approximate way by assuming some form for the velocity profile. This was attempted by Kurihara (1946) and Tani (1949) and is analogous to some approaches to flow in inclined channels (see e.g. Whitham 1974). A major problem for the Kurihara–Tani theory is, however, the lack of asymptotic steady-state solutions. In the inclined channel a steady-state solution is easily found by balancing the projection of gravity along the channel against the viscous damping, but in the radial case (with no inclination) the theory breaks down at a certain radius. Outside this radius there are no well-behaved asymptotic solutions.

The lack of asymptotic solutions turns out to be a very general phenomenon not specifically related to the Tani–Kurihara theory. If we assume that the velocity becomes small at some radius much larger than the jump radius, we can linearize the Navier–Stokes equations (in the boundary-layer approximation), and we then find that there are no asymptotic solutions. In fact, a stronger statement can be proved: within the full nonlinear boundary-layer theory and with some rather mild assumptions about the velocity, there are no asymptotic radially spreading solutions (Putkaradze & Rugh 1992). Of course, any real system is finite and we shall show in §3 that the outer solution becomes physically meaningful if we regard the point at which it becomes singular as corresponding to the edge of the plate, where the fluid drops off.

A closer look at the hydraulic jump suggests that it is not as simple as it appears. Experimental work by Tani (1949) and Craik *et al.* (1981) has shown that the jump region contains an eddy, whose inner edge determines the position of the jump. Other experiments (Watson 1964; Olsson & Turkdogan 1966; Nakoryakov, Pokusaev & Troyan 1978; Ishigai *et al.* 1977) also show that the flow is more complicated than the ideal version described above. This is also borne out in detailed simulations (Khalifa & McCorquodale 1992) of the jump region. At large flow rates, the flow becomes turbulent and the jump becomes ill defined and strongly fluctuating, including substantial breaking of the radial symmetry. In the following we shall restrict our attention to the laminar state which is found at small flow rates. Here the flow appears to be stationary and the jump is experimentally very well defined. We believe that our version of shallow-water theory can capture the rough features of this flow, although it does not take into account appropriately the separation which very likely occurs in the boundary layer (Bowles & Smith 1992). Thus the use of shallow-water theory prevents us from studying the detailed flow in the jump region, which, in our theory, is represented by a stationary shock.

The layout of the paper is as follows. Section 2 is devoted to ideal shallow-water theory for a radially symmetric system. Our main conclusion is that the ideal shallow-water equations do not allow a determination of the position of the hydraulic jump. Thus we turn in §3 to the viscous theory. Section 3.1 introduces the boundary-layer equations for this problem and in §3.2 the viscous shallow-water equations are obtained by averaging. It is noted that they do not allow decaying asymptotic solutions as $r \to \infty$. In §3.3 we show that the lack of decaying asymptotic solutions can be seen directly from the boundary-layer equations in their linearized form. We are then ready in §3.4 for the determination of the position of the hydraulic jump within viscous shallow-water theory and we compare our predictions with experiments. Finally, §3.5 deals with extensions of shallow-water theory in the presence of additional pressure drops.

2. Ideal shallow-water flow

We will first consider an ideal fluid. Since the thickness of the flow is everywhere very small and purely radial, we shall attempt to describe it with the shallow-water equations. (The accuracy of these equations is discussed in Courant & Friedrichs 1948, for example.) The equations for such a flow are

$$\frac{\partial v}{\partial t}+v\frac{\partial v}{\partial r}=-g\frac{\partial h}{\partial r}, \tag{1}$$

$$\frac{\partial h}{\partial t}+\frac{1}{r}\frac{\partial}{\partial r}\{rhv\}=0, \tag{2}$$

where $v(r,t)$ is the radial velocity, $h(r,t)$ is the height of the fluid, and g is the acceleration due to gravity. These two equations can be combined and rewritten as follows:

$$\frac{\partial}{\partial t}\{hv\}+\frac{1}{r}\frac{\partial}{\partial r}\{rh(v^2+\tfrac{1}{2}gh)\}=\frac{gh^2}{2r}, \tag{3}$$

$$\frac{\partial}{\partial t}\{\tfrac{1}{2}h(v^2+gh)\}+\frac{1}{r}\frac{\partial}{\partial r}\{rhv(\tfrac{1}{2}v^2+gh)\}=0. \tag{4}$$

Equations (2) and (4) describe conservation of volume and energy, respectively. Equation (3) is the equation of motion for the radial momentum, which is not conserved.

For a stationary flow the shallow-water equations become

$$v\frac{\mathrm{d}v}{\mathrm{d}r}=-g\frac{\mathrm{d}h}{\mathrm{d}r}, \tag{5}$$

$$\frac{1}{r}\frac{\mathrm{d}}{\mathrm{d}r}\{rhv\}=0. \tag{6}$$

Upon integration, we find

$$rhv=Q/2\pi \tag{7}$$

$$\tfrac{1}{2}v^2+gh=Q_e/Q, \tag{8}$$

where Q is the volume flux and Q_e is the energy flux per unit mass density. With the substitution

$$r=\tilde{r}\frac{gQ}{\pi}\left(\frac{2Q_e}{Q}\right)^{-\frac{3}{2}},\quad h=\tilde{h}\frac{1}{2g}\left(\frac{2Q_e}{Q}\right),\quad v=\tilde{v}\left(\frac{2Q_e}{Q}\right)^{\frac{1}{2}}, \tag{9}$$

(7) and (8) can be written in the dimensionless form

$$\tilde{r}\tilde{h}\tilde{v}=1, \tag{10}$$

$$\tilde{v}^2+\tilde{h}=1. \tag{11}$$

The solution to (10) and (11) can be written as

$$\tilde{r}=\frac{1}{\tilde{v}(1-\tilde{v}^2)}. \tag{12}$$

A plot of this function is shown in figure 1. It should be noted that there is a minimum

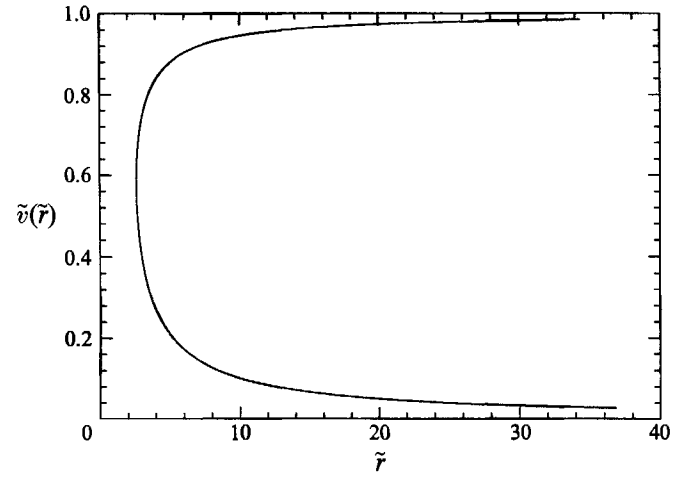

FIGURE 1. Solution for $\tilde{v}(\tilde{r})$ from (12) using the inviscid shallow-water equations.

radius $\tilde{r}_{min} = \frac{3}{2}\sqrt{3}$ below which there are no physical solutions. Thus, there are two continuous stationary solutions of the radial shallow-water equations with different asymptotic (large r) behaviour: $v \to$ const and $v \sim 1/r$. These solutions seem to agree with the observed behaviour before and after the jump, respectively (Olsson & Turkdogan 1966).

Equations (2)–(4) imply the following continuity conditions across a stationary discontinuity in the flow (Whitham 1974):

$$[vh] = 0, \tag{13}$$

$$[h(v^2 + \tfrac{1}{2}gh)] = 0, \tag{14}$$

$$[hv(\tfrac{1}{2}v^2 + gh)] = 0, \tag{15}$$

where the square brackets denote the difference of the enclosed quantities across the discontinuity. These equations are identical to those obtained in the channel flow problem (Rayleigh 1914). Even though the radial momentum is not conserved during the flow, it is still continuous across the jump since the right-hand side of (3) contains no derivatives (see e.g. Whitham 1974). Obviously, all three conditions cannot be satisfied simultaneously. If we assume continuity of volume and momentum flux, there must be a discontinuity in the energy flux per unit mass density given by

$$Q_{e2} - Q_{e1} = -\frac{gQ}{8\pi}\frac{(h_2 - h_1)^3}{h_1 h_2}, \tag{16}$$

where the subscripts 1 and 2 refer to the values of the associated quantities on either side of the discontinuity. Thus, if $h_2 > h_1$, the difference is negative, i.e. energy is dissipated at the jump. Also, since the energy loss is a monotonic function or r, there is apparently no special radius that might indicate the position of the discontinuity. Watson (1964) uses the conservation laws for mass and momentum flux to determine the position of the jump but requires knowledge of the height after the jump as an additional parameter.

It is often stated that the position of the jump can be found from the requirement that the fluid should be critical at the jump, meaning that the fluid velocity v should equal the velocity of gravity waves on the surface. Using the Froude number $Fr = v^2/gh$, we see from (12) that criticality ($Fr = 1$) implies that $\tilde{r} = \tilde{r}_{min}$. Furthermore,

the upper branch of $v(r)$ in figure 1 is always supercritical ($Fr > 1$) and the lower subcritical ($Fr < 1$), so the criterion of criticality cannot be used to determine the position of the jump.

3. Viscous theory

As seen in the last section, there seems to be no way of obtaining the jump from an inviscid theory. When one includes viscosity, a new and obvious reason for an instability in the flow appears. If we assume that the flow inside the jump has a constant surface velocity and decaying height as seen in experiments (Olsson & Turkdogan 1966), a very large shear stress builds up as the layer becomes thinner. This effect is accurately taken into account in the boundary-layer approximation (see e.g. Schlichting 1968), where it is assumed that vertical velocities are small compared to radial velocities and that the vertical variations (through the layer) are much more rapid than those in the radial direction.

3.1. *Boundary-layer equations*

In cylindrical coordinates, the equations of motion of the fluid in the boundary-layer approximation are

$$u\frac{\partial u}{\partial r}+w\frac{\partial u}{\partial z}=-g\frac{\mathrm{d}h}{\mathrm{d}r}+\nu\frac{\partial^2 u}{\partial z^2}, \tag{17}$$

$$\frac{\partial u}{\partial r}+\frac{u}{r}+\frac{\partial w}{\partial z}=0, \tag{18}$$

with the boundary conditions

$$\left.\begin{aligned} &u(r,0)=0, \quad w(r,0)=0,\\ &\frac{\partial u}{\partial z}\bigg|_{z=h(r)}=0, \quad r\int_0^{h(r)}u(r,z)\,\mathrm{d}z=q. \end{aligned}\right\} \tag{19}$$

Now, $u(r,z)$ is the radial component of the velocity, $w(r,z)$ is the vertical component, and $q=Q/2\pi$.

The boundary conditions (19) are not complete. We must cut off the equations at some radius $r=r_0$ larger than the jet radius, since at smaller radii the flow will be strongly affected by the vertical motion of the jet. Thus we must specify the radial velocity profile and the height at $r=r_0$:

$$u(r_0,z)=u_0(z), \quad h(r_0)=h_0. \tag{20}$$

Equations (17)–(19) can be rewritten in dimensionless form with the substitution

$$\left.\begin{aligned} u&=\alpha\tilde{u}, \quad \alpha=q^{\frac{1}{8}}\nu^{\frac{1}{8}}g^{\frac{3}{8}},\\ w&=\beta\tilde{w}, \quad \beta=q^{-\frac{1}{4}}\nu^{\frac{3}{4}}g^{\frac{1}{4}},\\ r&=\gamma\tilde{r}, \quad \gamma=q^{\frac{5}{8}}\nu^{-\frac{3}{8}}g^{-\frac{1}{8}},\\ z&=\delta\tilde{z}, \quad \delta=q^{\frac{1}{4}}\nu^{\frac{1}{4}}g^{-\frac{1}{4}}. \end{aligned}\right\} \tag{21}$$

Dropping the tilde, the rescaled equations are then

$$u\frac{\partial u}{\partial r}+w\frac{\partial u}{\partial z}=-\frac{\mathrm{d}h}{\mathrm{d}r}+\frac{\partial^2 u}{\partial z^2}, \tag{22}$$

$$\frac{\partial u}{\partial r}+\frac{u}{r}+\frac{\partial w}{\partial z}=0, \tag{23}$$

with the boundary conditions:

$$\left.\begin{aligned} &u(r,0)=0, \quad w(r,0)=0, \\ &\left.\frac{\partial u}{\partial z}\right|_{z=h(r)}=0, \quad r\int_0^{h(r)} u(r,z)\,\mathrm{d}z=1, \quad u(r_0,z)=\frac{u_0(z)}{\alpha}. \end{aligned}\right\} \tag{24}$$

The cutoff radius r_0 is chosen close to the vertical jet and therefore the velocity profile is assumed to be nearly constant, i.e. $u_0(z)=u_0$, since the boundary layer has not yet developed. Thus the boundary conditions depend essentially on a single parameter $\lambda = u_0/\alpha$.

3.2. *Viscous shallow-water flow*

To make further progress, we shall use a mean-value approach by averaging over the height of the fluid layer. Integrating (22) and (23) with respect to z and using the identity

$$\int_0^h w\frac{\partial u}{\partial z}\mathrm{d}z = h'u^2|_{z=h}+\int_0^h u\left(\frac{\partial u}{\partial r}+\frac{u}{r}\right)\mathrm{d}z, \tag{25}$$

we obtain the following equations:

$$\overline{u\frac{\partial u}{\partial r}} = -\frac{\mathrm{d}h}{\mathrm{d}r}-\frac{1}{h}\left.\frac{\partial u}{\partial z}\right|_{z=0}, \tag{26}$$

$$\bar{u}rh = 1, \tag{27}$$

where the bar denotes an average over z: $\bar{f}(r) = (1/h)\int_0^h f(r,z)\,\mathrm{d}z$.

We now make the following approximations:

$$\overline{\frac{\partial}{\partial r}u^2} = c_1\frac{\partial}{\partial r}v^2, \quad \left.\frac{\partial u}{\partial z}\right|_{z=0} = c_2\frac{v}{h}, \tag{28}$$

where $v=\bar{u}$, and c_1 and c_2 are dimensionless constants of order unity. For a parabolic profile, for example, $c_1=\frac{6}{5}$ and $c_2=3$. Substituting (28) into (26) and (27), and again rescaling such that $v\to c_1^{-\frac{1}{2}}c_2^{\frac{1}{2}}v$, $r\to c_1^{\frac{1}{2}}c_2^{-\frac{3}{8}}r$, and $h\to c_2^{\frac{1}{4}}h$, we now obtain

$$vv'+h' = -v/h^2, \tag{29}$$

$$vhr = 1, \tag{30}$$

which are equivalent to the equations derived by Kurihara (1946) and Tani (1949). The corresponding equations for momentum and energy are now

$$\frac{1}{r}\frac{\mathrm{d}}{\mathrm{d}r}\{rh(v^2+\tfrac{1}{2}h)\} = \frac{h^2}{2r}-\frac{1}{h^2r}, \tag{31}$$

$$\frac{1}{r}\frac{\mathrm{d}}{\mathrm{d}r}\{rhv(\tfrac{1}{2}v^2+h)\} = -\frac{1}{r^2h^3}. \tag{32}$$

Combining (29) and (30) leads to

$$v'\left(v-\frac{1}{v^2r}\right) = \frac{1}{vr^2}-v^3r^2. \tag{33}$$

A numerical solution of (33) leads to the typical integral curves shown in figure 2. These curves have in fact been obtained by solving the parametric equations:

$$\frac{\mathrm{d}r}{\mathrm{d}s} = v^3r^2-r, \quad \frac{\mathrm{d}v}{\mathrm{d}s} = v-v^5r^4, \tag{34}$$

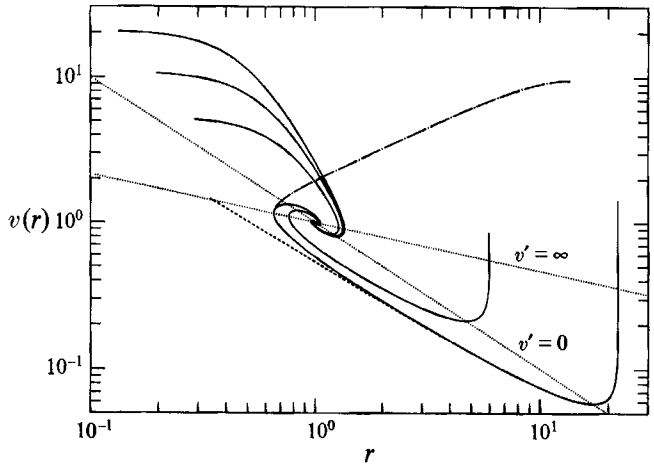

FIGURE 2. Integral curves (solid lines) showing the solutions to (34). The dashed line is the linearized approximation (36) for the outermost solution. The dotted lines show where $v'(r)$ is infinite and zero. The dot-dashed line is the jumpline for the outermost solution, i.e. the corresponding solution to (46).

and thus only segments where v is a unique function of r correspond to solutions of (33). The equations (34) have a focal point at $(r, v) = (1,1)$. This focus is the intersection of two curves: $v = r^{-\frac{1}{3}}(v' = \infty)$ and $v = r^{-1}(v' = 0)$. It can be shown that (33) has no physical solutions as $r \to \infty$. This follows from a theorem due to Hardy (1912) (see also Bellman 1970) regarding differential equations of the form,

$$y' = \frac{f(x,y)}{g(x,y)},$$

where $f(x,y)$ and $g(x,y)$ are polynomial functions of both arguments. Hardy showed that such equations have only continuous asymptotic behaviour of the form $r^a(\log r)^{1/n}$ or $e^{p(r)}r^b$, where n is an integer and $p(r)$ is a polynomial. It is easy to check that (33) does not have asymptotic behaviour of either of these forms and thus has none whatsoever. The behaviour at large r can be understood by trying the ansatz $v = y/r$ in (34). This leads to

$$\frac{dr}{ds} = \frac{y^3}{r} - r, \quad \frac{dy}{ds} = -y^5 + \frac{y^4}{r^2}, \tag{35}$$

and when the terms containing $1/r$ and $1/r^2$ are neglected, the two equations become independent. Their solutions are $r = r_0 e^{-s}$ and $y = (4s + y_0^{-4})^{-\frac{1}{4}}$, which can be combined to give

$$v = y/r = (1/r)[(r_0 v_0)^{-4} - 4\log(r/r_0)]^{-\frac{1}{4}}. \tag{36}$$

This approximate solution cannot be extended to infinity. For any choice of r_0 and v_0 it will diverge at $r_s = r_0 e^{\frac{1}{4}(r_0 v_0)^{-4}}$ with the form

$$v = (1/r)[4\log(r_s/r)]^{-\frac{1}{4}}. \tag{37}$$

One such solution is shown as the dashed line in figure 2. It should be noted that it follows the real solution rather accurately until fairly close to the focus even though the values of r are not very large. In reality v does not diverge but $v'(r)$ does diverge. In the parametric representation the integral curves turn around making it impossible to continue out to infinity (as seen from (35)).

3.3. *The lack of asymptotic states*

We shall now argue that the singular behaviour at $r \to \infty$ is not an artifact arising from the averaging over z. The same boundary-layer equations themselves display singular behaviour. Let us first rewrite the rescaled boundary-layer equations (22) and (24) in terms of the stream function $\Psi(r, z)$ defined by the relations

$$u = \frac{1}{r}\frac{\partial \Psi}{\partial z}, \quad w = -\frac{1}{r}\frac{\partial \Psi}{\partial r}, \tag{38}$$

which ensures that the continuity equation (23) is identically satisfied. Equation (22) then becomes

$$\frac{1}{r}\frac{\partial \Psi}{\partial z}\frac{\partial}{\partial r}\left(\frac{1}{r}\frac{\partial \Psi}{\partial z}\right) - \frac{1}{r}\frac{\partial \Psi}{\partial r}\frac{\partial}{\partial z}\frac{1}{r}\frac{\partial \Psi}{\partial z} = -\frac{dh}{dr} + \frac{1}{r}\frac{\partial^3 \Psi}{\partial z^3}, \tag{39}$$

with the boundary conditions

$$\left.\begin{aligned} &\Psi(r, 0) = 0, \quad \left.\frac{\partial \Psi}{\partial z}\right|_{z=0} = 0, \\ &\Psi(r, h) = 1, \quad \left.\frac{\partial^2 \Psi}{\partial z^2}\right|_{z=h(r)} = 0. \end{aligned}\right\} \tag{40}$$

Well beyond the hydraulic jump we now look for slowly decaying solutions where, at large enough radii, all velocities become small. At large distances such solutions should satisfy the linearized version of (39), but we shall see below that the linearized equations do not admit nice solutions as $r \to \infty$ and this contradicts our assumption concerning the existence of such decaying solutions. The linearized boundary-layer equation is

$$\frac{dh}{dr} = \frac{1}{r}\frac{\partial^3 \Psi}{\partial z^3}. \tag{41}$$

It follows from this equation that Ψ is a cubic function of z. The first two boundary conditions of (40) imply that it has the form $\Psi = f(r)\, z^2 + \frac{1}{6} r h' z^3$, where the functions $f(r)$ and $h(r)$ are to be determined using the two remaining boundary conditions. Thus,

$$\tfrac{1}{6} r h' h^3 + f(r)\, h^2 = 1, \quad r h' h + 2 f(r) = 0, \tag{42}$$

and finally we find a differential equation for h only:

$$h' h^3 = -3/r, \tag{43}$$

with the solution

$$h = (c - 12 \log r)^{\frac{1}{4}}. \tag{44}$$

The corresponding solution for Ψ is

$$\Psi = \tfrac{1}{2}(3\xi^2 - \xi^3), \tag{45}$$

where $\xi = z/h$.

The solution (44) is, except for a constant factor, identical to the solution (36) of the shallow-water equations. Again $h = 1/rv$ vanishes at some finite radius r_s and is not defined beyond that. This means, of course, that the linearization of (39) (i.e. neglecting the first term) which was made in order to obtain (44) breaks down as r approaches r_s and that our assumption that the velocities remain small is no longer valid. It can be shown that if the approximate solution (41) is used close to r_s, the neglected nonlinear terms of (39) would diverge as $(r_s - r)^{-\frac{3}{2}}$ and thus invalidate the solution. Therefore, the

linearized equations tell us nothing about the nature of the singularity nor do they strictly prove that a singularity exists. For a restricted class of solutions it is known, however, that the singular behaviour is not remedied by taking into account the nonlinear terms in (39): for any solution which is analytic in z and $1/r$, the height must vanish for some finite r (Putkaradze & Rugh 1992). The precise nature of this singularity is, however, not known. It should be noted that similar behaviour occurs for the linearized theory in channel flow. There the only difference is that the factor $1/r$ in (41) is missing. In this case, h will be a linear function of r and thus again vanishes at some finite radius.

At first sight this lack of asymptotic solutions seems strange and unphysical. In fact, however, the hydraulic jump usually appears under conditions that do not allow simple asymptotic states. In a kitchen sink there is a backflow, and in a typical experiment the fluid only spreads to the end of a plate, where it then falls off. In the latter case, one might approximate the flow very closely by a solution where h vanishes at the outer edge. The linearized solution (44) (with the constant c chosen such that $h \to 0$ at the edge of the plate) will then give an approximate solution except near the outer edge. We shall consider this possibility further in the next section.

One should note that the lack of asymptotic states depends crucially upon the effect of gravity. Watson (1964) neglects gravitational effects and thus obtain states where $v \sim r^{-3}$ and $h \sim r^2$. He argues that the effect of gravity is small in the thin layer between the jet and the jump. This is, as we have shown, not true well beyond the jump.

The boundary-layer approximation keeps only the 'transverse' viscous effects due to the rapid changes in the velocity field through the boundary layer. One can easily incorporate the 'longitudinal' effects in the shallow-water approach by adding the term $\nu(v'' + v'/r - v/r^2)$ to the right-hand side of the non-rescaled version of (33). This neither changes the spiralling nature of the integral curves leading to the breakdown of the inner solutions and, thus, to a sharp shock, nor produces asymptotic outer solutions. The same is true for surface-tension effects.

3.4. *Scaling of the hydraulic jump*

We have seen that although (33) has no real asymptotic solutions, it has well-defined outer solutions extending out to any given radius. In particular, for any radius r_s, there is a solution for which $v'(r) \to \infty$ precisely at $r = r_s$, which, for large r, is given approximately by (37). In experiments, a stationary flow is usually maintained by letting the fluid drop off the edge of a circular plate having a radius much larger than the jump radius. If we identify the edge with the limiting radius r_s, we have a unique outer solution which depends on the flow rate only through the rescaling factors. It will have essentially constant height until $r \approx r_s$, which is what we should expect.

The inner solutions are likewise only defined in a limited range. As seen in figure 2, they will start spiralling in toward the focus at $(r, v) = (1, 1)$ or, more precisely, $v'(r) \to -\infty$ at some point $r > 1$. It now seems reasonable to determine the entire flow by fitting a shock which connects the inner and the outer solution as shown in figure 3. Since the equations for energy and momentum flux (31) and (32) contain no extra derivatives, the matching should still be done according to (13) and (14). If we denote the rescaled velocities before and after the jump as v_1 and v_2 respectively, then they will be related by the equation

$$v_1 = \frac{1}{4v_2^2 r}[1 + (1 + 8v_2^3 r)^{\frac{1}{2}}] \tag{46}$$

(which is symmetric under interchange of v_1 and v_2).

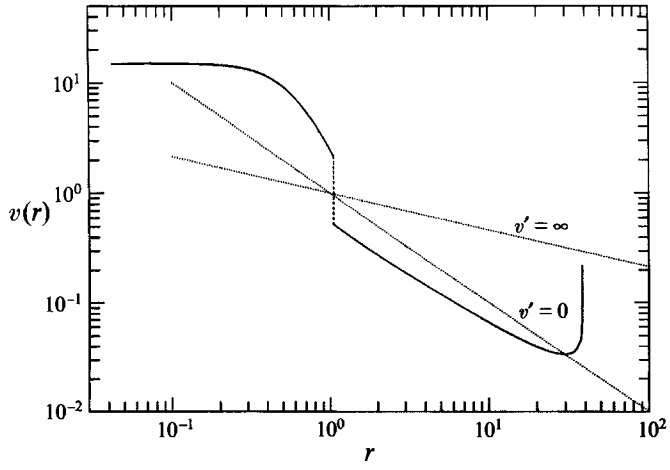

FIGURE 3. The jump is interpreted as a discontinuity (dashed line) connecting the inner and outer solutions (solid lines) shown in figure 2. The jump does not pass through the focus, although it may appear to do so.

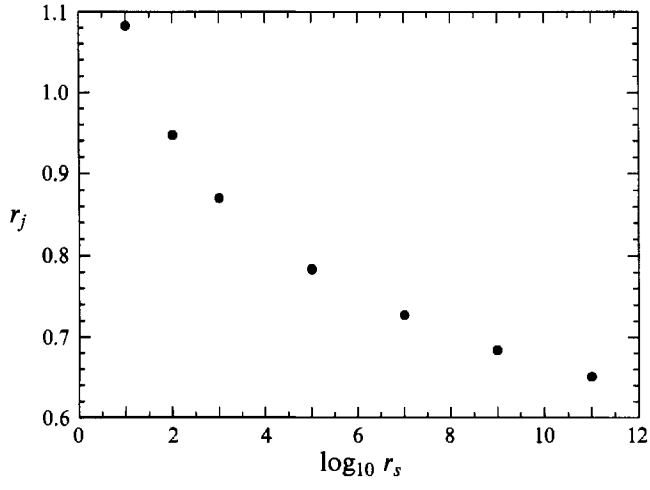

FIGURE 4. The dependence of the position of the jump r_j on the singularity at r_s.

The choice of outer solution depends on r_s as noted above, but the dependence is very weak as seen in figure 2. Small changes in v_2 right after the jump have a strong effect on r_s which follows from the approximate solution (37), which can be inverted to give

$$r_s \approx e^{\frac{1}{4}v_2^4}, \tag{47}$$

where v_2 denotes the outer solution at $r = 1$. This means that no matter which large r_s we choose, the outer solution will remain almost unchanged. Figure 2 shows the outermost solution with its corresponding jumpline (i.e. the solution of (46)) for $r_s = 20.3$. The jump occurs when the inner solution crosses this line. The spiralling nature of the inner solution and the large power of v appearing in (34) imply that, independently of the initial conditions chosen for the inner solution, the jump always occurs close to $r = 1$, as seen in figure 2. As noted earlier, the exact location of the jump does depend on r_s. The dependence is, however, extremely weak as seen in figure 4. Here we show the dependence of r_j on r_s for a typical inner solution. One can see that

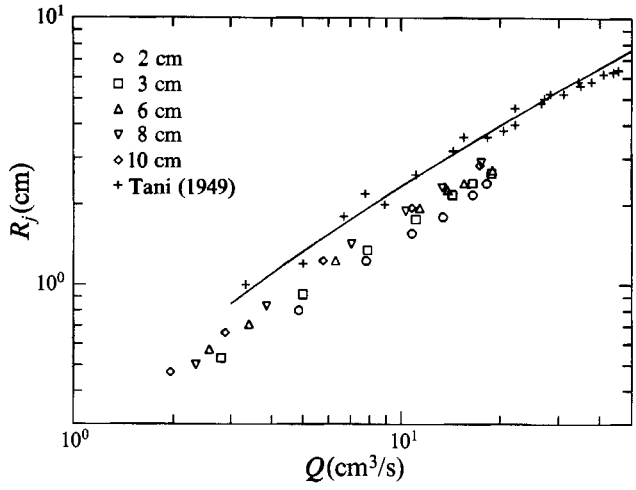

FIGURE 5. Experimental data for the position of the jump R_j as a function of flux Q (from Dimon *et al.* 1992). The different data sets are for different nozzle heights (see text). Data from Tani (1949) are also shown. The solid line is the theoretical prediction for the position of the jump.

we have to increase r_s many orders of magnitude to have any significant effect on r_j. Thus, as long as $r_s \gg r_j$ (but not astronomical), there is a strong selection of $r_j \approx 1$, which means that the physical (i.e. non-rescaled) jump radius R_j scales as (21):

$$R_j \approx \gamma = cq^{\frac{5}{8}}\nu^{-\frac{3}{8}}g^{-\frac{1}{8}}, \tag{48}$$

where the constant c depends on the velocity profile chosen in (28). For a parabolic profile, which we shall assume for definiteness, $c \approx 0.73$.

To compare more directly with experiments, we have computed $R_j(Q)$ for a range of Q with the (non-rescaled) value of the edge radius (radius of the plate) R_s fixed and with a particular set of initial conditions for u. Fixing R_s means that r_s depends on Q as $r_s = R_s/\gamma$. With $c \approx 0.73$ for a parabolic profile and $\nu = 0.01$ cm^2/s, we find,

$$r_s \approx 1.8Q^{-\frac{5}{6}}R_s \tag{49}$$

in c.g.s units. For the inner boundary conditions, we have assumed that the shape of the spreading jet is independent of Q, which means that the physical velocity V at a fixed point R_0 varies linearly with Q:

$$V(R_0) = \frac{Q}{2\pi H_0 R_0}, \tag{50}$$

where H_0 is the height of the fluid layer at $r = R_0$, which is assumed to be independent of Q. The scaled boundary conditions are then found from $V(R_0) = \alpha v(1.8Q^{-\frac{5}{8}}R_0)$ or

$$v(1.8Q^{-\frac{5}{8}}R_0) = \frac{1}{H_0 R_0}q^{\frac{7}{8}}\nu^{-\frac{1}{8}}g^{-\frac{3}{8}} \sim \frac{1}{H_0 R_0}0.027Q^{\frac{7}{8}}. \tag{51}$$

In figure 5 we show data from Dimon *et al.* (1992) for the radius of the hydraulic jump as a function of flux when the flow is stationary. In this experiment, a jet of water from an 8 mm diameter nozzle impinges on a plate 40 cm in diameter. A small amount of soap (0.04% by volume) was added to the water to facilitate even wetting of the plate. The flux was controlled with a constant-head tank and measured directly at the nozzle. The range in Q corresponds to $1 < Fr(R_0) < 80$. The jump radius was

determined with a precision telescope. The height of the nozzle was varied to see the effect of changing the boundary condition $H_0(R_0)$. A typical value is $H_0 = 0.05$ cm when $R_0 = 1$ cm (which is also comparable with the values measured by Olsson & Turkdogan 1966). Using this value and $R_s = 20$ cm, we have computed the corresponding jump radius R_j which is also shown in figure 5. With the above boundary condition, the theoretical curve cannot be continued below $Q \approx 3$ cm^3/s since R_j will become less than R_0. The theoretical curve is not strongly sensitive to the specific choice of H_0. Variations in H_0 by a factor of two up or down only changes R_j on the order of 10%. A fit to the experimental data with the power law $R_j \sim Q^\kappa$ yielded $0.75 < \kappa < 0.82$ over the different data sets shown. Similar scaling is found for the computed R_j ($\kappa \approx 0.75$). We also include older data from Tani (1949) for comparison. The deviation of the exponent κ from $\frac{5}{8}$ in (48) can be thought of as a finite size effect. In other words, we believe that the apparent power laws seen in figure 5 are not really asymptotic, but are affected by correction terms to (48).

The results from the theory are surprisingly good considering the many approximations made in order to obtain the shallow-water equation (33). In this equation, both the longitudinal viscosity terms and the surface tension are neglected. As noted earlier, they do not change the qualitative behaviour (i.e. they do not smooth out the jump in the simplified theory), but they might modify the effective exponents seen at small Q. Also, the choice of boundary conditions is a possible source of error. When the fluid strikes the horizontal surface, a very complicated process takes place which is not well understood. In order to use boundary-layer theory, one must assume that the vertical velocity components are small compared to the horizontal components. This is certainly not the case close to the impinging jet and it is not clear precisely where it becomes valid. More fundamentally, the averaging performed in (28) becomes invalid if the boundary-layer undergoes separation. Tani (1949) assumed that the ratio of w to u is linear in z and showed that the boundary-layer equations then lead to separation at some radius. The same scaling (48) holds for this separation radius, since his solution for the velocity profile is only valid if the velocity profile at the inlet is also of this form, and then both the equations and the boundary conditions can be rescaled according to (21). The belief that separation occurs near the jump is further supported by recent work (Bowles & Smith 1992) and, as noted in the Introduction, this makes it clear that our approximate theory can only be used well beyond the jump region.

3.5. *Inclusion of an additional pressure drop*

It is interesting to note that if the flow is subjected to an additional pressure gradient not of the boundary-layer–hydrostatic type, the problems connected with the lack of asymptotic states may disappear. This can happen if, for example, the plate is curved. If such pressure gradients do not fall off too slowly, they regularize the problem by ensuring that asymptotic states exists. This is clear in the one-dimensional problem of flow down an inclined channel (Whitham 1974; Pumir, Manneville & Pomeau 1983). There the balance between the slope and the viscous damping produces a steady mean flow.

It is easy to test the consequences of an additional pressure drop. Let us assume, for example, that an additional pressure gradient $p \sim \mu r^{-\eta}$ is acting at large r. If we insert this additional term in the linearized boundary-layer equation (41), we find, instead of (43), the expression

$$(h' - \mu r^{-\eta}) h^3 = -3/r. \tag{52}$$

For any $\eta < 1$, the additional term dominates and we get the regular asymptotic behaviour $h(r) \to r^\alpha$ where $\alpha = \frac{1}{3}(\eta - 1)$.

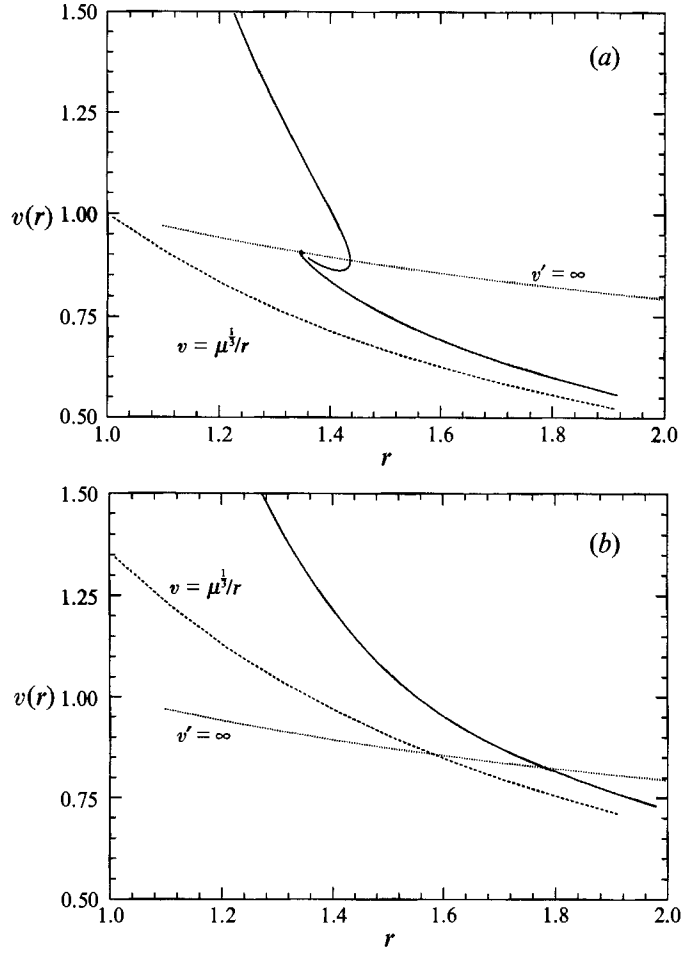

FIGURE 6. Integral curves (solid lines) with the additional pressure term included for (*a*) $\mu = 1$ and (*b*) $\mu = 2.5$. The dashed lines show the asymptotic (large r) solution.

The same relations hold for the shallow-water equation (33). Inserting an extra pressure gradient as above leads to the equation

$$v'\left(v-\frac{1}{v^2 r}\right) = \frac{1}{vr^2} - v^3 r^2 + \mu r^{-\eta}, \tag{53}$$

and again if $\eta < 1$, there are asymptotic solutions. In figure 6 we show numerical solutions of (53) with $\eta = 1$, and (*a*) $\mu = 1$ and (*b*) $\mu = 2.5$. For $\mu = 1$, the inner solutions still spiral although an outer solution now exists all the way to infinity. For larger μ, the spiralling disappears and we find a smooth kink-like solution connecting the two states. The behaviour around the focal point (which shifts with μ) changes from damped to overdamped oscillations, and for large μ, the solution passes right through the fixed point without spiralling.

We would like to thank Robert MacKay for stirring our interest in this problem. We further acknowledge helpful discussion with P. Dimotakis, C. Jayaprakash, H. J. Jensen, and Y. Pomeau. We also benefited from communications with R. Bowles and

E. Watson. T.B. thanks Novo's Foundation for support and P.D. thanks the SARC Foundation for support. V.P. is grateful to H. Topsøe for a Bohr-Kapitsa scholarship and to the Niels Bohr Institute for hospitality during his stay.

REFERENCES

BELLMANN, R. 1970 *Methods of Nonlinear Analysis*, vol. 1. Academic.

BOWLES, R. I. & SMITH, F. T. 1992 *J. Fluid Mech.* **242**, 145.

COURANT, R. & FRIEDICHS. K. O. 1948 *Supersonic Flows and Shock Waves*. Interscience.

CRAIK, A. D. D., LATHAM, R. C., FAWKES, M. J. & GRIBBON, P. W. F. 1981 *J. Fluid Mech.* **112**, 347.

DIMON, P., ELLEGAARD, C., HANSEN, R. H., HØRLÜCK, S. & ZAUNER, D. 1992.

HARDY, G. H. 1912 *Proc. Lond. Math. Soc.* **10**, 451.

ISHIGAI, S., NAKANISHI, S., MIZUNO, M. & IMAMURA, T. 1977 *Bull. JSME* **20**, 85.

KHALIFA, A. A. M. & MCCORQUODALE, J. A. 1992 *J. Hydraul. Res.* **30**, 149.

KURIHARA, M. 1946 *Rep. Research Institute for Fluid Engng, Kyusyu Imperial University*, vol. 3, p. 11.

LANDAU, L. D. & LIFSHITZ, E. M. 1987 *Fluid Mechanics*. Pergamon.

NAKORYAKOV, V. E., POKUSAEV, B. G. & TROYAN, E. N. 1978 *Intl J. Heat Mass Transfer* **21**, 1175.

OLSSON, R. G. & TURKDOGAN, E. T. 1966 *Nature* **211**, 813.

PUMIR, A., MANNEVILLE, P. & POMEAU, Y. 1983 *J. Fluid Mech.* **135**, 27.

PUTKARADZE, V. P. & RUGH, H. H. 1992 *Proc. R. Soc. Lond.* A (to appear).

RAYLEIGH, LORD 1914 *Proc. R. Soc. Lond.* A **90**, 324.

SCHLICHTING, H. 1968 *Boundary Layer Theory*. McGraw-Hill.

TANI, I. 1949 *J. Phys. Soc. Japan* **4**, 212.

WATSON, E. J. 1964 *J. Fluid Mech.* **20**, 481.

WHITHAM, G. B. 1974 *Linear and Nonlinear Waves*. Wiley-Interscience.